SCIENCE CHINA
Chemistry

•ARTICLES•

https://doi.org/10.1007/s11426-020-9772-0

Bioactive polypeptide hydrogels modified with RGD and N-cadherin mimetic peptide promote chondrogenic differentiation of bone marrow mesenchymal stem cells

Yan Rong[1,2], Zhen Zhang[1,3], Chaoliang He[1,3*] & Xuesi Chen[1,3]

[1]*Key Laboratory of Polymer Ecomaterials, Changchun Institute of Applied Chemistry, Chinese Academy of Sciences, Changchun 130022, China;*
[2]*University of Chinese Academy of Sciences, Beijing 100039, China;*
[3]*University of Science and Technology of China, Hefei 230026, China*

Received April 7, 2020; accepted May 9, 2020; published online June 8, 2020

Cell-material and cell-cell interactions represent two crucial aspects of the regulation of cell behavior. In the present study, poly (L-glutamic acid) (PLG) hydrogels were prepared by catalyst-free click crosslinking *via* a strain-promoted azide-alkyne cycloaddition (SPAAC) reaction between azido-grafted PLG (PLG-N_3) and azadibenzocyclooctyne-grafted PLG (PLG-ADIBO). The bioactive peptides c(RGDfK) and N-cadherin mimetic peptide (N-Cad) were both conjugated to the PLG hydrogel (denoted PLG+RGD/N-Cad) in order to regulate cell-material and cell-cell interactions. Gelation time and storage modulus of the hydrogels were tunable through variations in the concentration of polypeptide precursors. The hydrogels degraded gradually in the presence of proteinases. The viability of bone marrow mesenchymal stem cells (BMSCs) was maintained when cultured with extracts of the hydrogels or encapsulated within the hydrogels. Degradation was observed within 10 weeks following the subcutaneous injection of hydrogel solution in rats, displaying excellent histocompatibility *in vivo*. The introduction of RGD into the PLG hydrogel promoted the adhesion of BMSCs onto the hydrogels. Moreover, when encapsulated within the PLG+RGD/N-Cad hydrogel, BMSCs secreted cartilage-specific matrix, in addition to chondrogenic gene and protein expression being significantly enhanced in comparison with BMSCs encapsulated in hydrogels without N-Cad modification. These findings suggest that these biodegradable, bioactive polypeptide hydrogels have great potential for use in 3D cell culture and in cartilage tissue engineering.

polypeptide hydrogel, click crosslinking, biofunctionalization, 3D cell culture, tissue engineering

Citation: Rong Y, Zhang Z, He C, Chen X. Bioactive polypeptide hydrogels modified with RGD and N-cadherin mimetic peptide promote chondrogenic differentiation of bone marrow mesenchymal stem cells. *Sci China Chem*, 2020, 63, https://doi.org/10.1007/s11426-020-9772-0

1 Introduction

Hydrogels are a class of three-dimensional hydrophilic or amphiphilic polymer network with a large proportion of their volume consisting of water. Because of their viscoelastic properties and high water content, hydrogels are considered potential scaffolds that mimic natural extracellular matrix (ECM) for tissue engineering applications [1–5]. A number of naturally-derived polymers and biodegradable synthetic polymers have been studied as building blocks for hydrogel formation due to their good biocompatibility and biodegradability [6–9]. The advantages of synthetic polymers lie in their defined composition and chemical structure, in addition to tunable mechanical properties [8,10]. Synthetic polypeptides are a type of unique biodegradable synthetic polymer composed of natural α-amino acid residues, which

*Corresponding author (email: clhe@ciac.ac.cn)

show excellent biocompatibility, biodegradability, and biomimetic secondary structure similar to that of natural proteins. In addition, the inherent carboxyl, amino or hydroxyl side groups of some polypeptides facilitate additional incorporation of functional moieties [11–14]. Thus, polypeptide hydrogels have recently been investigated as emerging scaffolds for 3D cell culture and tissue engineering applications [15–20]. For instance, in previous studies, we and other groups, have developed poly(L-glutamic acid) (PLG)-based hydrogels with adjustable mechanical properties for encapsulation of bone marrow mesenchymal stem cells (BMSCs) and chondrocytes [16,21].

Additionally, many crosslinking approaches have been utilized to fabricate covalently-crosslinked networks of hydrogels. In previous studies, polypeptide hydrogels crosslinked *via* a horseradish/hydrogen peroxidase (HRP/H_2O_2) system, hydrazone formation reaction, and an *N*-(3-dimethylaminopropyl)-*N*′-ethylcarbodiimide hydrochloride/*N*-hydroxysuccinimide (EDC/NHS) system, have been developed as tissue engineering scaffolds [13,16,21]. However, crosslinking systems involving H_2O_2, free radicals, aldehydes or small-molecule chemical crosslinking agents may cause potential toxicity towards the encapsulated cells. Recently, bioorthogonal reactions, especially catalyst-free click reactions, have attracted considerable attention as emerging crosslinking strategies due to their speed, efficiency and high selectivity, in addition to their excellent biocompatibility both *in vitro* and *in vivo* [22–24]. For example, it has been reported that bone marrow stromal cells encapsulated in poly(ethylene glycol)-*co*-polycarbonate hydrogels crosslinked using a strain-promoted azide-alkyne cycloaddition (SPAAC) reaction displayed greater cellular viability than those encapsulated in photo-crosslinked poly(ethylene glycol) dimethacrylate (PEG-DMA) hydrogels [25].

The biofunctionality of hydrogels is also a crucial factor that significantly affects tissue regeneration in addition to the method used in cross-linking. Based on the interactions between materials and cells, considerable effort has been devoted to the design of materials that actively communicate with complex biological environments [15,26–28]. The conjugation of bioactive factors is a facile and effective way to impart biological function to synthetic materials. RGD, a cell binding domain that is found in fibronectin (FN), laminin (LN) and collagen, is the most commonly used cell-adhesive peptide. A total of 24 integrins bind to ECM molecules in an RGD-mediated manner [29,30]. It has been reported that, compared with linear RGD, cyclic RGD (cRGD) exhibits stronger affinity to integrin with greater biological activity [31]. Furthermore, neural cadherin (N-cadherin) is considered an important factor for regulating cell differentiation by directing cell-cell interactions during mesenchymal condensation and chondrogenesis [32,33]. The intercellular communication is mediated through the homotypic interaction of N-cadherin on adjacent mesenchymal cells. N-cadherin contains an extracellular domain responsible for its homotypic binding as well as a cytosolic domain to bind the actin cytoskeleton through the catenin family [32,34]. Previous studies have shown that synthetic mimetic peptides containing the His-Ala-Val (HAV) domain, an evolutionarily conserved motif in the first extracellular domain (ECD1) of N-cadherin, have similar binding properties to N-cadherin [35,36]. Bian *et al.* [37] and Burdick *et al*. [38–40] have reported that a self-assembled peptide hydrogel and a hyaluronic acid (HA) hydrogel grafted with the N-cadherin mimetic peptide promoted chondrogenic differentiation of mesenchymal stem cells (MSCs). Hydrogels that incorporate cues for both matrix-cell and cell-cell interactions may represent a new paradigm in scaffolds that regulate MSC differentiation. Nevertheless, to date, hydrogels capable of both promoting cell adhesion on materials and regulating cell-cell interactions are rarely reported.

In the present work, an injectable PLG hydrogel crosslinked *via* a catalyst-free SPAAC reaction between azido and dibenzocyclooctyne groups was developed under physiological conditions. Both c(RGDfK) and a N-cadherin mimetic peptide (N-Cad) were conjugated to the PLG network in order that the hydrogel could regulate cell proliferation and differentiation (Figure 1). Gelation time, mechanical properties and degradation properties of the hydrogels were investigated. The biocompatibility of hydrogels was evaluated both *in vitro* and *in vivo* and the proliferation of cells encapsulated in the hydrogels measured. Furthermore, the accumulation of cartilage-specific matrix and the expression of chondrogenic markers on BMSCs encapsulated in the biofunctionalized hydrogels were studied.

2 Materials and methods

2.1 Materials

γ-Benzyl-L-glutamate-*N*-carboxyanhydride (BLG NCA) was synthesized in accordance with a previously published method [41]. EDC (Aladdin, 98%), 4-dimethylaminopyridine (DMAP, Aladdin, 99%, USA), NHS (Aladdin, 98%), c(RGDfK) (GL Biochem, 95%), N-cadherin mimetic peptide (Ac-HAVDIGGGK, GL Biochem, 95%, China), Scrambled peptide (Ac-AGVGDHIGK, GL Biochem, 95%) and azadibenzocyclooctyne-ethylamine•TFA (ADIBO-NH_2•TFA, Biomatrik, China) were used as received. Azide-substituted diethylene glycol (EG_2N_3) was prepared by the reaction of sodium azide (NaN_3, Multipoint Chem, 98%) with 2-(2-chloroethoxy)ethanol (Adamas, 98%), in accordance with a previously-published method [42]. Tetrahydrofuran (THF) and *N*,*N*-dimethylformamide (DMF) were dried over magnesium sulfate prior to use. Dulbecco's modified eagle medium: nutrient mixture F-12 (DMEM/F12) was purchased

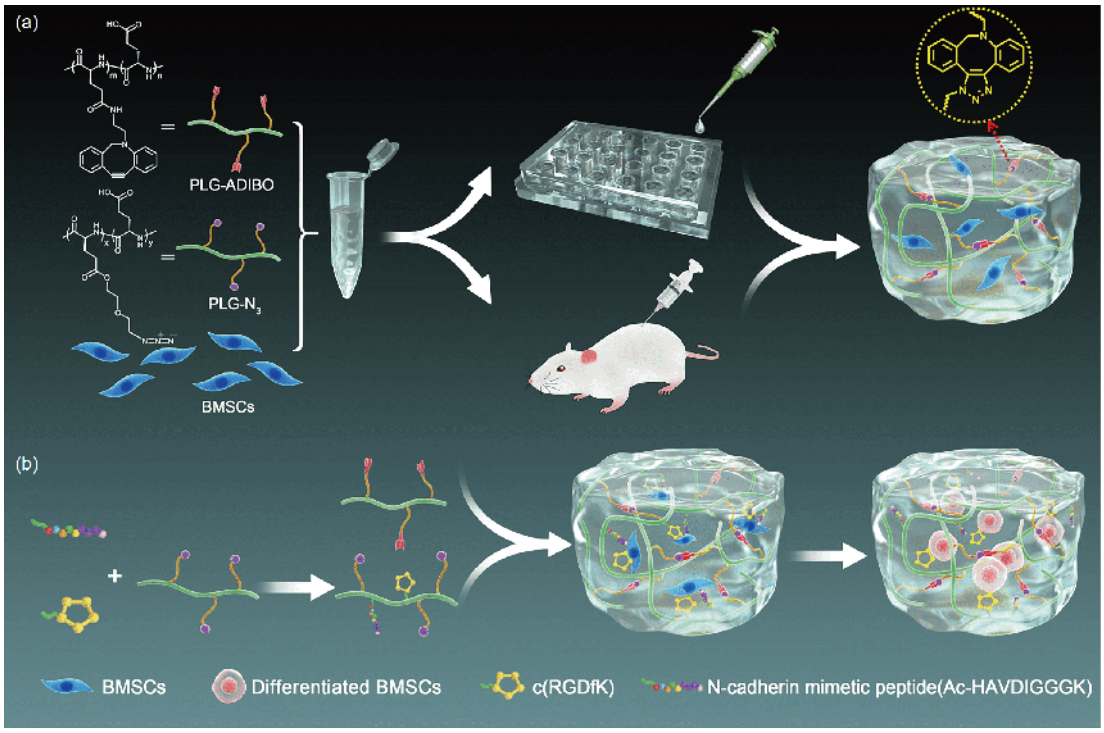

Figure 1 (a) Schematic diagram of the formation of click-crosslinked polypeptide hydrogels from PLG-N_3 and PLG-ADIBO for use as a cell delivery vehicle. (b) Bioactive c(RGDfK) and N-cadherin mimetic peptides introduced into the PLG backbone to construct bioactive polypeptide hydrogels (color online).

from Gibco. Elastase (4.6 U/mg) was purchased from Worthington and transforming growth factor-β1 (TGF-β1) was obtained from PeproTech (USA). Insulin-transferrin-sodium selenite media supplement (ITS), papain (30 U/mg), proteinase K (30 U/mg) and 1,9-dimethyl-methylene blue (DMMB) were acquired from Sigma-Aldrich (USA).

2.2 Characterization

Proton nuclear magnetic resonance (^{1}H NMR) spectra were recorded using a Bruker AV 500 NMR spectrometer (Germany) in deuterium oxide (D_2O), deuterated trifluoroacetic acid (CF_3COOD) or deuterated chloroform ($CDCl_3$). The molecular weights and polydispersity indexes (PDI) were measured by gel permeation chromatography (GPC) on a Waters 1515 Isocratic HPLC pump equipped with Ultrahydrogel™ linear column and a Waters 2414 refractive index detector (USA). The eluant was 0.2 M phosphate buffer (PB) containing 0.1 M $NaNO_3$ and 0.2 g/L NaN_3. The flow rate was 0.6 mL/min and the testing temperature was 35 °C. Monodisperse polyethylene glycol (PEG, Waters Co. Ltd., USA) with molecular weights ranging from 1,000 to 2.18×10^5 were used as the standards for generating the calibration curve. The grafting ratio of c(RGDfK) was measured by using a Perkin-Elmer LS50B luminescence spectrometer (USA). The fluorescence excitation spectra were recorded at the detection wavelength of 395 nm. The grafting ratio of N-cadherin mimetic peptide and scrambled peptide was determined by measuring the absorbance at 420 nm with an ultraviolet-visible (UV-Vis) spectrophotometer (UV-2401PC, Shimadzu, Japan). Scanning electron microscopy (SEM) was performed on a scanning electron microscope (Merlin, Zeiss, Germany).

2.3 Synthesis of PLG-ADIBO, PLG-N_3, and peptide-modified PLG-N_3

PLG was prepared in accordance with a method we previously reported [41]. Briefly, BLG NCA was dissolved in anhydrous DMF under an atmosphere of nitrogen and an appropriate quantity of *n*-hexylamine added. The mixture was stirred at room temperature for 3 d and the resultant poly (γ-benzyl-L-glutamate) (PBLG) was purified by precipitation into diethyl ether, filtration then vacuum drying. The PBLG obtained in this way (6 g) was dissolved in dichloroacetic acid (60 mL) then 33% hydrobromic acid in acetic acid (20 mL) was added to the solution. The deprotection reaction of PBLG was allowed to proceed whilst stirring at room temperature for 2 h, and the product of the reaction obtained by precipitation into diethyl ether and filtration. Crude PLG was purified by dissolution in DMF, dialysis against deionized water and lyophilization.

ADIBO-modified PLG (PLG-ADIBO) was synthesized by coupling PLG with ADIBO-NH_2•TFA *via* an EDC/NHS-mediated amidation reaction. PLG was dissolved in DMF and EDC then NHS was added (EDC:NHS:–COOH=2:2:10, molar ratio) to activate a proportion of the carboxyl groups.

ADIBO-NH_2 was then added (ADIBO:–COOH=1:10, molar ratio) and the mixture stirred at room temperature in the dark for 3 d. The resultant PLG-ADIBO was dialyzed against deionized water then lyophilized.

Azido-modified PLG (PLG-N_3) was synthesized by coupling PLG with 2-(2-azidoethoxy)ethanol *via* an EDC/DMAP-mediated coupling reaction. PLG was dissolved in DMF and 2-(2-azidoethoxy)ethanol was added (N_3:–COOH=1:10, molar ratio). After several minutes, EDC and DMAP were added (EDC:DMAP:–COOH=2:0.2:10, molar ratio), after which the mixture was stirred at room temperature for 3 d. The resultant PLG-N_3 was dialyzed against deionized water then lyophilized.

RGD and N-cadherin mimetic peptide (N-Cad)-modified PLG-N_3 (denoted PLG-N_3/RGD/N-Cad) was obtained by successively coupling PLG-N_3 with c(RGDfK) and N-Cad using an EDC/NHS-mediated amidation reaction. Following the dissolution of PLG-N_3 in DMF, EDC and NHS were added (EDC:NHS:–COOH=4:4:100, molar ratio) and the solution stirred at room temperature for 1 d. The product was precipitated in diethyl ether, washed with ethanol, collected by centrifugation and dried under vacuum. The resultant product was then dissolved in DMF. c(RGDfK) and N-Cad were added and the mixture was stirred at room temperature for 3 d (c(RGDfK):N-Cad:–COOH=1:1:100, molar ratio). The resultant PLG-N_3/RGD/N-Cad was dialyzed against deionized water then lyophilized. Finally, a control sample was fabricated by synthesis of RGD and scrambled peptide (Scram)-modified PLG-N_3 (denoted PLG-N_3/RGD/Scram) using a similar method, but with Scram substituted in place of N-Cad.

The grafting ratio of each molecule was ascertained by ^{1}H NMR. The content of RGD was rechecked by measuring arginine content, as previously reported [43]. The concentration of N-cadherin mimetic peptide and scrambled peptide were rechecked using the Pauly reaction [44] (Figure S1(a, b), Supporting Information online).

2.4 Hydrogel formation

PLG-ADIBO, PLG-N_3, PLG-N_3/RGD/N-Cad and PLG-N_3/RGD/Scram were dissolved separately in phosphate buffered saline (PBS, 0.01 M) at predetermined concentrations. PLG hydrogels with and without peptide modification were then formed by mixing PLG-ADIBO with PLG-N_3, PLG-N_3/RGD/N-Cad or PLG-N_3/RGD/Scram at an N_3/ADIBO molar ratio of 1:1. Specifically, the PLG hydrogels without peptide modification were prepared by mixing PLG-ADIBO with PLG-N_3. The PLG hydrogels modified with RGD and N-Cad (denoted PLG+RGD/N-Cad) were prepared by mixing PLG-ADIBO with PLG-N_3/RGD/N-Cad. The PLG hydrogels modified with RGD and Scram (denoted PLG+RGD/Scram) were prepared by mixing PLG-ADIBO with PLG-N_3/RGD/Scram.

Gelation time was measured using a vial tilting method. When no flow was observed 30 s after inversion of the vial, the sample was regarded as having formed a gel.

2.5 Morphology of hydrogels

SEM was employed for observation of morphology of the PLG hydrogel. The samples were frozen in liquid nitrogen and subsequently lyophilized for 3 d. The specimens were sectioned and cross sections were coated with gold. Morphology of the PLG hydrogel was measured on a scanning electron microscope.

2.6 Mechanical characterization

Rheological tests were conducted on an MCR302 Rheometer containing a 25 mm parallel plate at 37 °C. Briefly, once mixtures of PLG-N_3 and PLG-ADIBO at different concentrations had been prepared, samples were immediately deposited into a 500 μm gap between two parallel plates of a rheometer. Time-dependent storage modulus (G') and loss modulus (G'') were measured at a constant frequency of 1 Hz and strain of 1%.

2.7 *In vitro* hydrogel degradation

Degradation of the hydrogels was evaluated by incubating 0.1 mL hydrogel in 1 mL 0.01 M PBS with or without an enzyme at 37 °C. To assess enzymatic degradation, proteinase K (5 U/mL) or elastase (5 U/mL) was added to samples then refreshed every day. The mass of the gel was weighed daily until the samples were completely degraded.

2.8 *In vitro* cytocompatibility

Rabbit BMSCs were expanded to passage 3 using growth media (DMEM/F12 with 10% FBS, 50 U/mL penicillin and 50 μg/mL streptomycin). BMSCs were seeded into the wells of 96-well plates at a density of 1×10^4 cells/well in 0.1 mL of media for 24 h. The media was subsequently replaced with 0.1 mL of extract (DMEM/F12, 37 °C, 72 h) of the PLG-N_3/PLG-ADIBO hydrogel. Fresh media and PEI 25K (0.125 mg/mL) were used as negative and positive controls, respectively. After 24 h of incubation, cells were incubated with media containing 3-(4,5-dimethylthiazol-2-yl)-2,5-diphenyltetrazolium bromide (MTT) (1 mg/mL) for 4 h after which the absorbance at 490 nm was measured using a microplate reader (Tecan Spark, Switzerland).

The viability of BMSCs within hydrogels was evaluated as follows. BMSC-encapsulated hydrogels were obtained by mixing PLG-N_3 and PLG-ADIBO solutions with a cell suspension under sterile conditions at 37 °C. The final con-

centration of cells and hydrogels was adjusted as required. The morphology of cells within the hydrogels was observed using actin and nuclear staining, as follows. BMSC-encapsulated hydrogels were prepared in glass bottom cell culture dishes (1.5×10^5 cells/mL). After 48 h, the samples were fixed using paraformaldehyde and stained firstly with Alexa Fluor 488 Phalloidin (30 min) then DAPI (1 μg/mL, 5 min). Cell morphology was imaged using confocal laser scanning microscopy (LSM 700, Zeiss). The viability of BMSCs in the hydrogels was assessed using live-dead cell staining. Briefly, the hydrogels (4×10^5 cells/mL) were stained at predetermined time points with 2 μM calcein-AM and 4.5 μM propidium iodine (PI) in 0.01 M PBS. The staining was performed at 37 °C in the dark for 45 min and the results were observed then imaged using a fluorescence microscope. For 3D views of confocal laser scanning microscopy images, the hydrogels (4×10^5 cells/mL) were stained at 48 h with 2 μM calcein-AM and 4.5 μM PI, and a 200 μm z-stack was acquired.

2.9 *In vivo* hydrogel degradation and biocompatibility

In vivo hydrogel degradation and biocompatibility were tested using a Sprague Dawley (SD) rat model (~200 g body weight). A 0.2 mL volume of 3% (*w*/*v*) hydrogel precursor solution was subcutaneously injected into the dorsal region of each rat which then underwent gelation. At predetermined time intervals (0, 1, 2, 4, 6, 8, 10 weeks), the animals were sacrificed and the remaining hydrogel collected then photographed. Tissue surrounding the hydrogel was harvested and fixed in 4% paraformaldehyde. Histopathological examination was performed after hematoxylin and eosin (H&E) staining of the tissue.

All animal experiments were approved and conducted in accordance with the guidelines of the Animal Experimental Center of Jilin University Institutional Animal Care and Use Committee.

2.10 Cell extraction, culture and induction

Rabbit BMSCs were isolated from 4-week-old New Zealand White rabbits using a whole bone marrow adherence method, as previously described [16]. Briefly, bone marrow from rabbit femurs was collected, filtered using 200 mesh, washed in PBS, then cultured in DMEM/F12 (50 U/mL penicillin, 50 μg/mL streptomycin, 10% FBS) medium for approximately 2 weeks. At an appropriate level of cell expansion, the cells were digested (0.25% trypsin) and passaged for subsequent use (Figure S2). Meanwhile, cartilage was obtained from rabbit knee joints and chondrocytes isolated by sequential trypsin and collagenase digestion. Chondrocyte media consisted of DMEM/F12, antibiotics (100 U/mL penicillin and 100 μg/mL streptomycin) and 10% FBS.

Chondrogenesis of BMSCs in 2D and 3D culture was achieved by incubation in induction media (DMEM/F12, 50 U/mL penicillin, 50 μg/mL streptomycin, 10 ng/mL TGF-β1, 1% ITS, 50 μg/mL ascorbate, 50 μg/mL L-proline, 0.1 μM dexamethasone, 0.9 mM sodium pyruvate). The media was replaced every three days.

2.11 Cell proliferation within hydrogels

Hydrogels containing cells were prepared using the same procedure as described above. The proliferation of BMSCs or chondrocytes within hydrogels (2×10^5 cells/mL) was measured using a cell counting kit-8 (CCK-8) assay. CCK-8 solution (10% *v*/*v*) was added to each sample at predetermined time points then incubated for 3 h. Absorbance at 450 and 630 nm (baseline correction) was then measured. Cells were cultured with proliferation medium (DMEM/F12, antibiotics and 10% FBS) at 37 °C and in an atmosphere containing 5% CO_2.

2.12 Glycosaminoglycan (GAG) production

After culturing for 3 weeks, hydrogels containing BMSCs (6×10^6 cells/mL) were lyophilized, the dry weight measured then digested with papain solution (5 U/mL) at 60 °C for 20 h. GAG production was quantified using a dimethylmethylene blue dye assay (DMMB) in accordance with a method described previously [15]. Chondroitin sulfate-A was used to generate a standard curve. dsDNA was quantified using PicoGreen reagent, in accordance with the manufacturer's instructions (Figure S1(c, d)).

2.13 RNA extraction and gene expression analysis

BMSC-laden hydrogels (1, 3, 7 d) were transferred into TRIzol reagent (Invitrogen, USA) then evenly ground to extract the RNA in accordance with the manufacturer's instructions, and then quantified using a microplate reader. RNA samples were reverse-transcribed into cDNA using HiScript III RT SuperMix for qPCR (+gDNA wiper) (Vazyme). Quantitative real-time polymerase chain reaction (qRT-PCR) was performed using a Mxpro3005P QPCR system (Stratagene, USA) with ChamQ SYBR Color qPCR Master Mix. Primer sequences are listed in Table S1 (Supporting Information online). Levels of gene expression were calculated using the $2^{-\Delta\Delta Ct}$ method and normalized against GAPDH (housekeeping gene).

2.14 Protein extraction and expression assessment

After 10 days of incubation, BMSC-laden hydrogels were ground and lysed in RIPA buffer (containing PMSF) at 4 °C. After quantification of protein concentration in samples

using a BCA kit (Thermo, USA), equal quantities of protein per sample were electrophoresed in 10% polyacrylamide gel then transferred to a polyvinylidene fluoride (PVDF) membrane. The membranes were blocked in Tris-buffered saline/Tween-20 (TBST) with 5% bovine serum albumin at room temperature for 1 h. The membranes were then incubated in fresh blocking buffer overnight at 4 °C with one of the following primary antibodies: ACAN Rabbit pAb (1:1,000, ABclonal), COL2A1 Rabbit pAb (1:1,000, ABclonal) or β-actin monoclonal antibody (1:2,000, rabbit, CST). Subsequently, the membranes were washed with TBST and incubated with goat anti rabbit IgG-HRP secondary antibody (1:2,000, ABclonal) at room temperature for 40 min. The membranes were then washed in TBST and bands were visualized by enhanced chemiluminescence (ECL) using a Western blotting substrate (Beyotime). The density of each protein band was measured using Image J software. β-actin represented the control.

3 Results and discussion

3.1 Synthesis and characterization of PLG-ADIBO, PLG-N_3, and peptide-modified PLG-N_3

The synthetic routes of PLG modification with N_3, ADIBO and peptides are displayed in Scheme 1. PLG was obtained by ring opening polymerization of BLG NCA, which was confirmed by ^{1}H NMR.

Based on the gel permeation chromatography test, the number-average molecular weight (M_n) of PLG was 18,900, with a PDI of 1.19. PLG-N_3 or PLG-ADIBO was then synthesized by grafting N_3- or ADIBO-bearing molecules to the carboxyl side groups of PLG *via* carbodiimide chemistry. To obtain PLG-N_3/RGD/N-Cad (or PLG-N_3/RGD/Scram), PLG-N_3 was additionally modified with amino-bearing c(RGDfK) and N-cadherin mimetic peptide (or scrambled peptide) using an EDC/NHS-mediated amidation reaction. The grafting ratios of target molecules were calculated as the number of grafted target groups per 100 L-glutamic acid residues based on ^{1}H NMR results (Figure 2, Table 1). ADIBO was grafted to PLG at a grafting ratio of approximately 6%, as determined by comparison of the integral of the phenyl peak at around 7.2 ppm with that of the methylene peak of the L-glutamate unit at around 4.3 ppm (Figure 2). Similarly, the grafting ratios of N_3, RGD, N-cadherin mimetic peptide (N-Cad) and scrambled peptide (Scram) were calculated as approximately 9%, 0.5%, 0.3%, and 0.3%, respectively (Table 1). Furthermore, the concentration of RGD was re-evaluated by measuring arginine content, resulting in a grafting ratio of 0.54%. N-cadherin mimetic peptide and scrambled peptide were retested using the Pauly reaction, which indicated grafting ratios of 0.33% and 0.35% (Figure

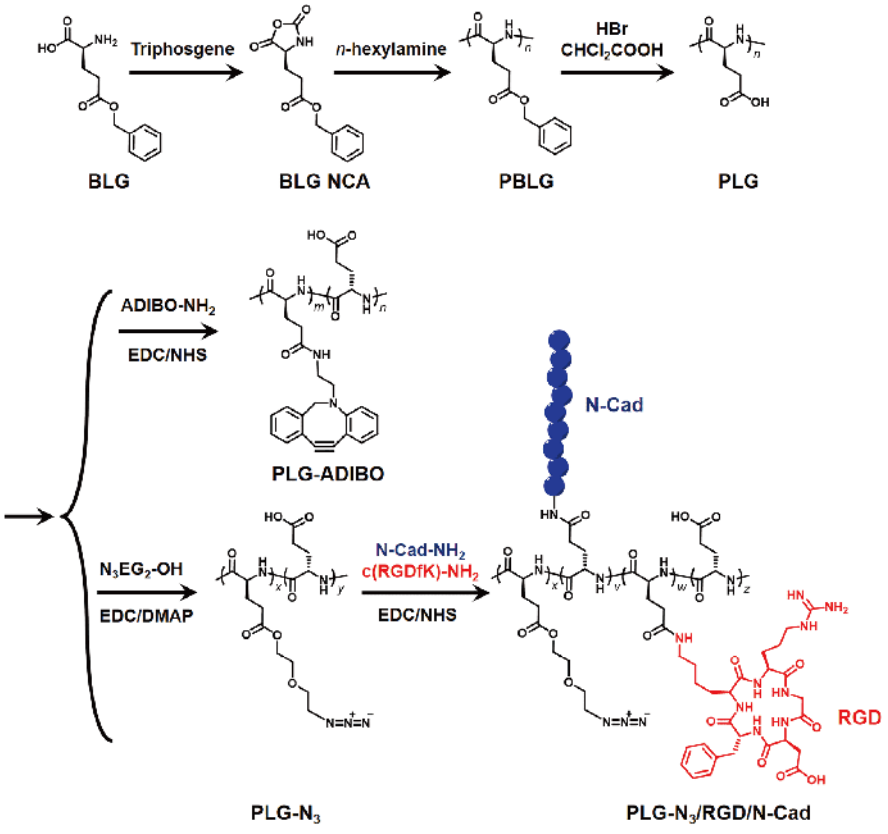

Scheme 1 Routes of synthesis of PLG-ADIBO, PLG-N_3 and PLG-N_3/RGD/N-Cad (color online).

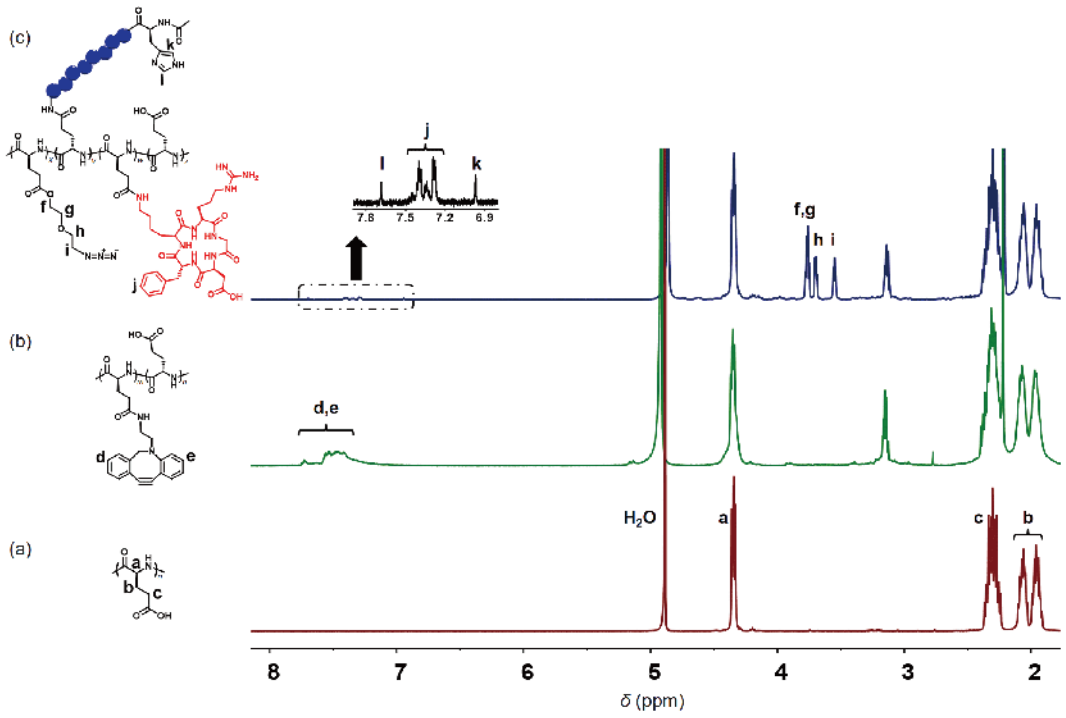

Figure 2 ^{1}H NMR spectra of PLG (a), PLG-ADIBO (b), PLG-N_3/RGD/N-Cad (c) in D_2O (color online).

Table 1 Reaction feeds, grafting ratios and grafting efficiencies of the PLG graft copolymers

Sample	Molecules to be grafted (X)[a)]	Reaction feed ratio: X/–COOH (mol/mol)	Grafting ratio[b)]	Grafting efficiency[b)]
PLG-ADIBO	ADIBO	1:10	6%	60%
PLG-N_3	N_3	1:10	9%	90%
PLG-N_3/RGD/Scram	RGD, Scram	1:100, 1:100	0.52%, 0.32%	52%, 32%
PLG-N_3/RGD/N-Cad	RGD, N-Cad	1:100, 1:100	0.49%, 0.3%	49%, 30%

a) X represents the molecule to be grafted; b) calculated by ^{1}H NMR.

S1(a, b)). Thus, the re-evaluated figures are consistent with the ^{1}H NMR data.

3.2 Preparation and characterization of the hydrogels

Transparent PLG-based hydrogels were formed by simply mixing PLG-N_3 and PLG-ADIBO in PBS at an N_3/ADIBO molar ratio of 1:1 without external stimulus or catalyst (Figure 3(a)). The rate of crosslinking was positively correlated with polymer concentration. When the concentrations of each were increased from 3% to 6% (*w*/*v*), gelation time of the hydrogels reduced markedly from 35 to 1.5 min, as measured using the vial inversion method (Figure 3(b)). Increased rate of gelation with increasing polymer concentration can be attributed to the greater concentrations of N_3 and ADIBO groups, which contributed to the crosslinking reaction [25]. Furthermore, the result of SEM showed that the PLG hydrogel had porous structure, which was conducive to the circulation of bioactive molecules (Figure 3(c)). In order to study the viscoelastic properties of the hydrogels, the storage modulus (G') and loss modulus (G'') during the gelation process were measured over time (Figure 3(d)). It was observed that, where the crosspoint of G' and G'' was considered the gelation point, the gelation time reduced with increasing polymer concentration from 3% to 6% (*w*/*v*). The results agreed well with those of the vial inversion test. Furthermore, G' at the plateau increased markedly from 300 to 9,400 Pa as polymer concentration increased from 3% to 6% (*w*/*v*), likely due to the increase in crosslinking density. It has been reported that hydrogels with relatively low crosslinking density are more conducive to maintaining stem cell viability and function [45–47], and so 3% (*w*/*v*) hydrogel was selected for the remaining cell studies. Additionally, the viscoelastic properties of hydrogels formed from PLG-ADIBO with PLG-N_3/RGD/N-Cad or PLG-N_3/RGD/Scram were also tested (Figure S3). The results indicate that PLG hydrogels with peptide modification exhibited comparable G' and G'' to the PLG hydrogel without peptide modification,

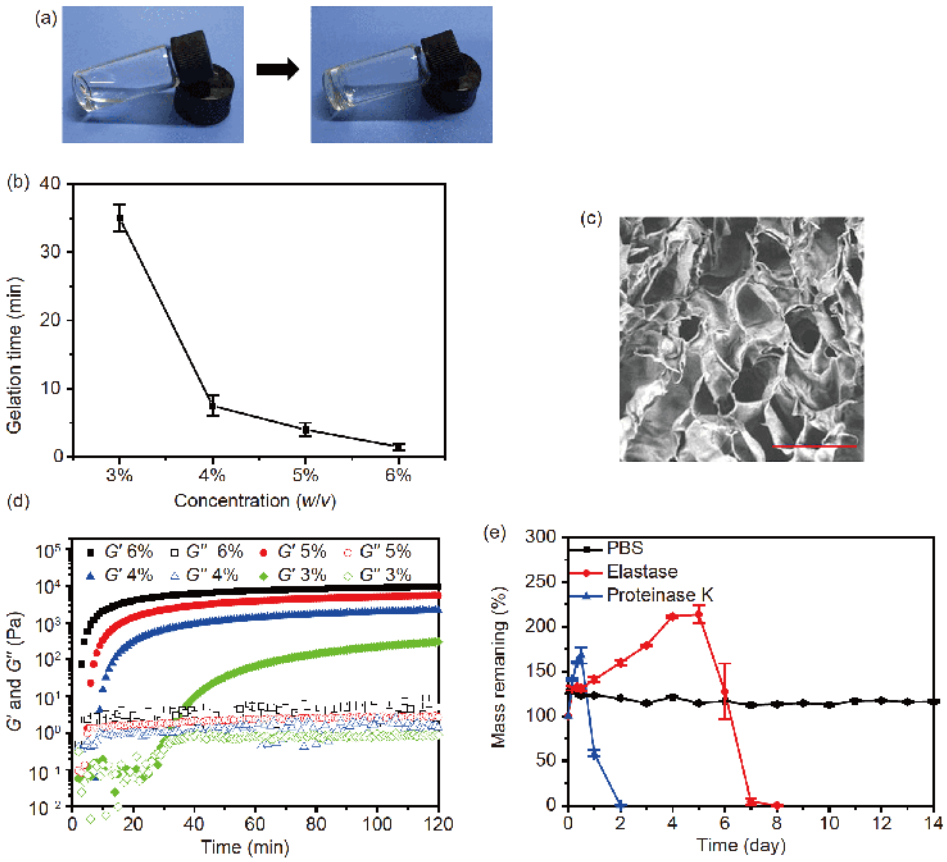

Figure 3 (a) Photographs of the sol-gel transition of 3% (*w*/*v*) PLG. (b) Gelation time of different concentrations of PLG hydrogels at 37 °C. (c) SEM image of lyophilized 3% (*w*/*v*) PLG hydrogels. Scale bar: 100 μm. (d) Storage modulus (*G*′) and loss modulus (*G*″) of PLG hydrogels with different concentrations as a function of time. (e) *In vitro* degradation profiles for the 3% (*w*/*v*) hydrogels incubated in 0.01 M PBS (pH 7.4) containing 5 U/mL proteinase K, 5 U/mL elastase, and PBS without any proteinase as control, respectively (n=3) (color online).

and so such differences are unlikely to cause additional interference to subsequent cell tests [48].

Degradation of the hydrogels *in vitro* was measured in the presence of proteinases at 37 °C. As shown in Figure 3(e), the hydrogels were relatively stable in PBS for 2 weeks, whereas degradation of the hydrogels occurred after addition of various proteinases. The gel samples degraded completely in approximately 7 days in the presence of elastase, but more rapidly, within 2 days, in the presence of protease K. Notably, the weight of the gels increased during the initial stages then decreased in solutions containing enzymes. This can reasonably be explained by the gradual cleavage of PLG-based networks leading to a decrease in crosslinking density and hydrogel swelling during the initial stage [17]. After integrity of the hydrogels could not be maintained during the later stages, the samples decomposed completely.

3.3 *In vitro* and *in vivo* biocompatibility

In vitro biocompatibility of the PLG hydrogel was evaluated by survival of the BMSCs. The cells were cultured with hydrogel extract (72 h, 37 °C) for 24 h then cell viability was measured by MTT, using PEI 25K (0.125 mg/mL) as a positive control. Cell viability in the presence of hydrogel extract was maintained above 90% (Figure 4(a)), indicating that the hydrogel exhibited no detectable cytotoxicity. BMSCs were additionally encapsulated in PLG hydrogels, and cell morphology and survival monitored. The hydrogels retained transparent during the experimental period of cell culture, which was beneficial to the observation of cell status within the hydrogels. Compared with the spreading observed on tissue culture plastic (TCP), BMSCs instead retained a spherical morphology when dispersed inside the hydrogels (Figure 4(b, c)), consistent with previously-published literature [49]. Moreover, live-dead staining of the cells indicated that the majority remained alive (stained green) after 14 days in culture (Figure 4(d)). The hydrogel demonstrated excellent biocompatibility *in vitro*, as shown by the results of cytotoxicity and 3D culture assay. The excellent cytocompatibility of the polypeptide hydrogel was likely due to the low cytotoxicity of PLG and the mild gelation process of the SPAAC reaction [24,50].

In vivo degradation and biocompatibility of the hydrogels were tested in a rat model. After mixing PLG-ADIBO and

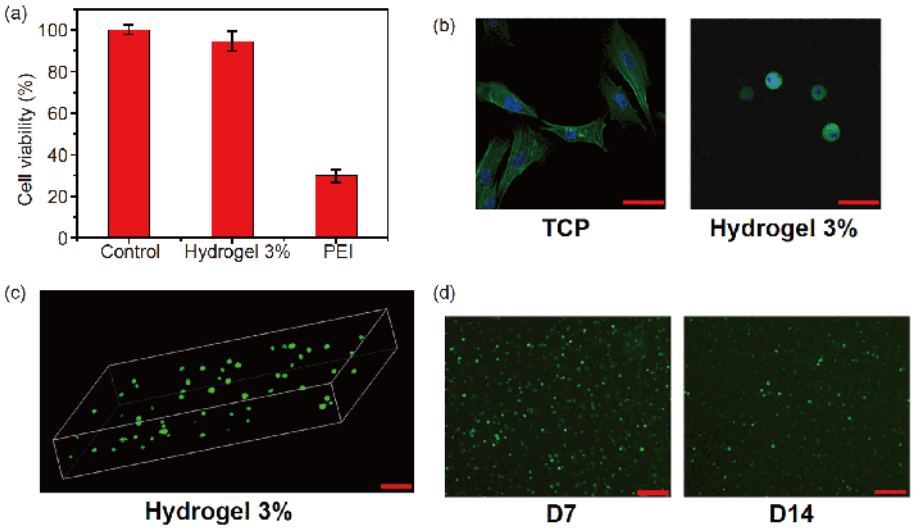

Figure 4 (a) Viability of BMSCs after exposure to the supernatant of 3% (*w*/*v*) PLG hydrogels for 24 h. PEI 25K was used as a positive control (n=3). (b, c) Confocal images of BMSCs after encapsulation in 3% (*w*/*v*) PLG hydrogels for 48 h: (b) cells were stained with Alexa Fluor 488-Phalloidin (F-actin, green) and DAPI (cell nuclei, blue). Scale bar: 50 μm; (c) cells were stained with calcein-AM and PI. Scale bar: 100 μm. (d) Live-dead cell staining of BMSCs in 3% (*w*/*v*) PLG hydrogels after incubation for 7 or 14 days. Cells were stained with calcein-AM (green, live) and PI (red, dead). Scale bar: 100 μm (color online).

PLG-N_3 with or without peptide modification for 10 min, mixtures of the 3% (*w*/*v*) precursor solutions were injected subcutaneously into the backs of rats for *in situ* gelation. Stable hydrogels were formed within several minutes, and the subcutaneous hydrogels degraded completely within 10 weeks.

The inflammatory reactions of the tissue surrounding the hydrogels were evaluated using H&E staining. A slightly increased accumulation of inflammatory cells was observed within 2 weeks following injection of the hydrogel, implying that a mild foreign body reaction had occurred [15]. It is noteworthy that the number of inflammatory cells in the vicinity decreased as gradual degradation of the hydrogels occurred, suggesting a gradual alleviation of the inflammatory reaction (Figure 5 and Figures S4, S5). After the complete degradation of the hydrogels, the inflammatory reaction disappeared. Furthermore, the presence of hydrogels caused no apparent necrosis, edema, hyperemia or hemorrhaging at the site of injection. The results above indicate that the PLG hydrogel was biodegradable and exhibited good biocompatibility *in vivo*.

3.4 Cell proliferation within hydrogels

The 3% (*w*/*v*) PLG hydrogel formed from PLG-N_3 and PLG-ADIBO was used as the scaffold for 3D cell culture, with cell proliferation measured using a CCK-8 assay. Chondrocytes that had been encapsulated in the hydrogels and cultured for a week, had proliferated continuously, as displayed in Figure 6(a). Notably, the BMSCs did not proliferate within the PLG hydrogels, as expected [51,52]. However, cell proliferation within c(RGDfK)-modified hydrogels increased somewhat (Figure 6(b)). It is noteworthy that, even though BMSCs maintained high survival rate, the proliferation of BMSCs within the hydrogels was slower than that of chondrocytes. This is probably attributed to the fact that BMSCs were more sensitive to the variation of microenvironment, leading to relatively slower proliferation rate. Similar results have been reported in some other systems, in which cells kept alive over long-term culture in hydrogels, but no significant proliferation was observed [53,54]. The adhesion promoting effect of RGD has been widely recognized. Song *et al.* [55] also established that hydrogels modified with RGD promoted the proliferation of MSCs within the gels. In the present study, the bioactivity of hydrogels also improved by the introduction of RGD. In addition, the surface adhesion of BMSCs on the hydrogels was measured using gradient RGD modified gels (Figure S6). It was found that the modification of PLG hydrogels with RGD (≥0.5 mM) promoted cell adhesion, with cell proliferation being significantly enhanced (Figure S7).

3.5 Differentiation of BMSCs into chondrocytes within the hydrogels

Chondrogenesis of BMSCs within the polypeptide hydrogel was induced using chondrogenic induction medium. The secretion of glycosaminoglycans (GAGs) is a characteristic of chondrocytes, so measurement of the accumulation of GAGs within the hydrogels is evidence of the differentiation of BMSCs into chondrocytes [56]. After incubation of BMSCs in hydrogels in the presence of chondrogenic induction medium for 3 weeks, the yield of GAGs was measured by DMMB and normalized to DNA content. As shown

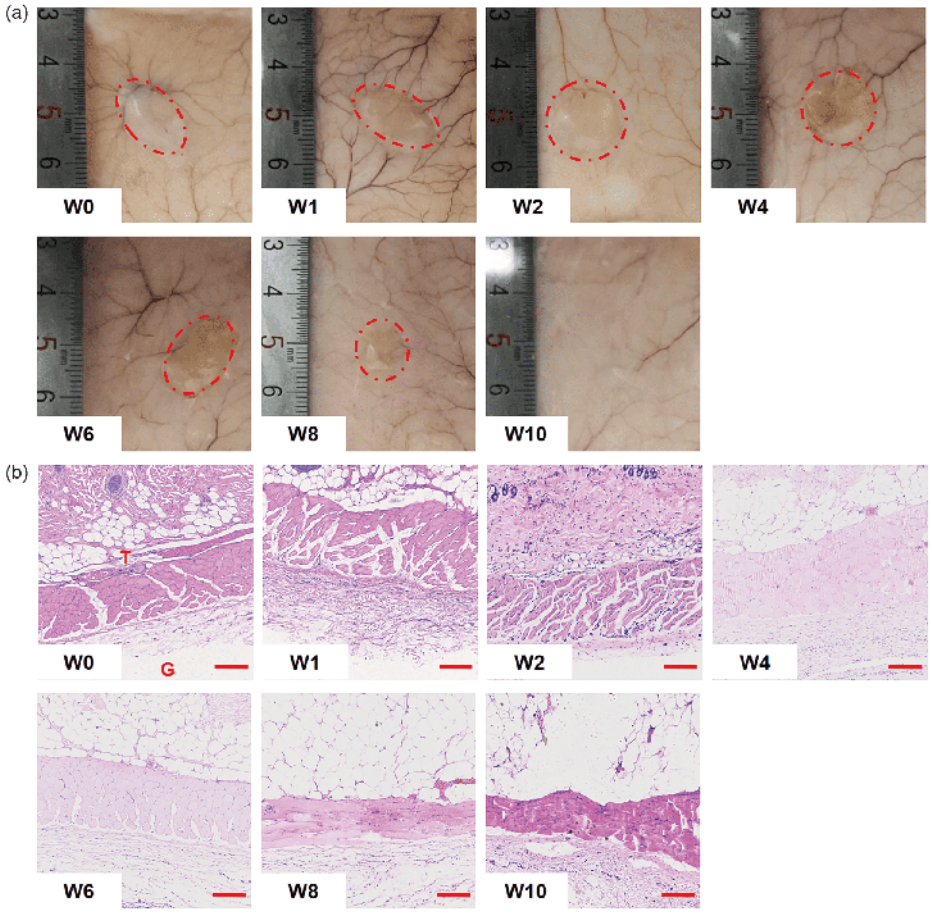

Figure 5 (a) *In vivo* implantation of 3% (*w*/*v*) PLG hydrogels after various time intervals. (b) H&E staining images of tissues surrounding the injection sites at different time periods. Scale bar: 100 μm (color online).

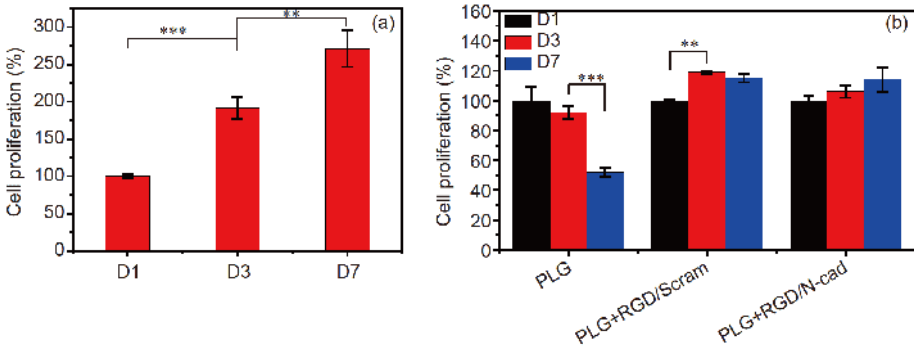

Figure 6 (a) Proliferation of chondrocytes encapsulated in 3% (*w*/*v*) PLG hydrogels as a function of time. (b) Proliferation of BMSCs within the three types of hydrogel: 3% (*w*/*v*) PLG hydrogels, 3% (*w*/*v*) PLG+RGD/Scram hydrogels, 3% (*w*/*v*) PLG+RGD/N-Cad hydrogels (n=3), (**p<0.01, ***p<0.001) (color online).

in Figure 7(a), the quantity of GAG generated by the cells within the PLG+RGD/N-Cad hydrogel was significantly higher than that secreted by cells in PLG and PLG+RGD/Scram hydrogels. The result indicates that the N-cadherin mimetic peptide promoted chondrogenic differentiation of BMSCs. Furthermore, similar results of gene and protein expression were obtained. It was found that the levels of aggrecan and type II collagen (collagen II) gene expression increased in all three groups during 1 week incubation in chondrogenic induction media (Figure 7(b, c)). However, the gene expressions of these markers of chondrogenic differentiation following culture in the PLG+RGD/N-Cad hydrogel were significantly higher than those in other groups. The Western blot (WB) bands indicated that protein expression of aggrecan and collagen II were also correspondingly enhanced in the hydrogel modified with N-cadherin mimetic

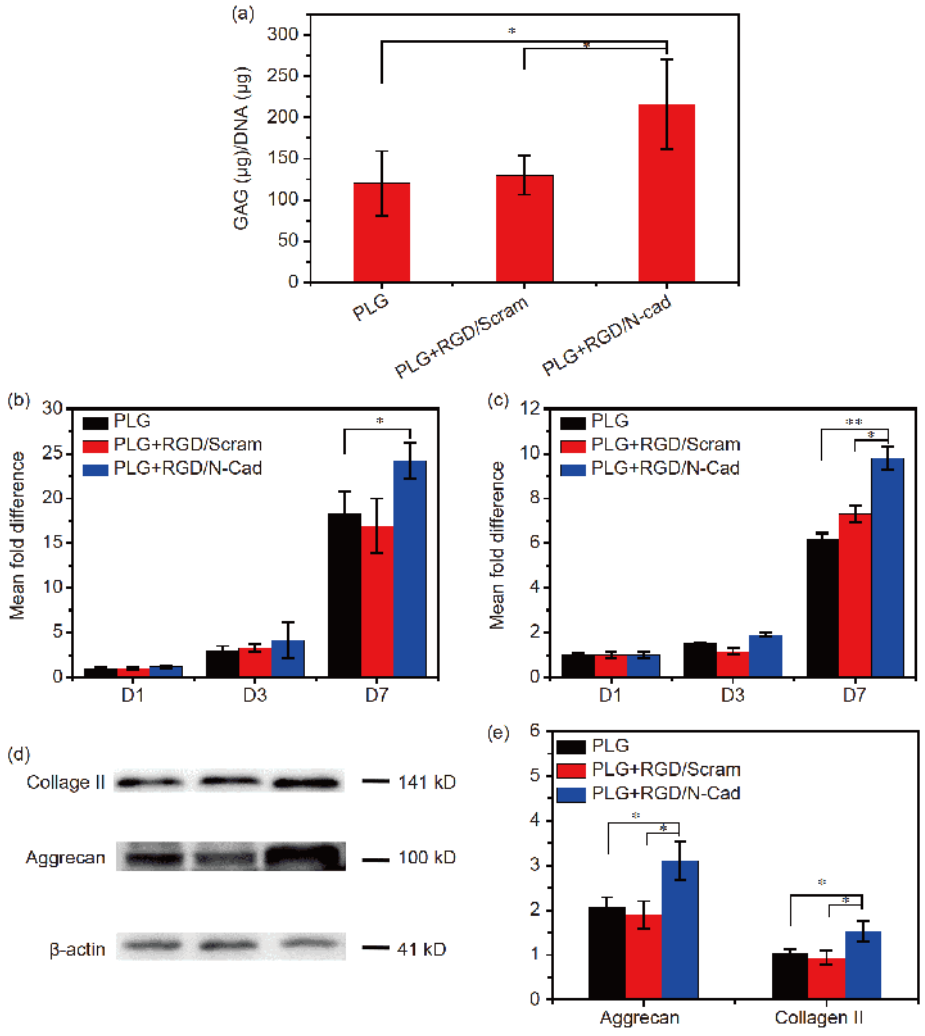

Figure 7 Chondrogenic differentiation of BMSCs in response to N-Cad-modified 3D hydrogels. (a) Quantification of GAG in hydrogels containing BMSCs after induction of chondrogenesis in culture for 3 weeks (normalized to DNA content). (b, c) Quantitative RT-PCR of aggrecan (b) and collagen II (c) in BMSCs within hydrogels during the first week of induced differentiation (normalized to the housekeeping gene GAPDH). (d, e) Representative Western blots for aggrecan and collagen II of BMSCs after induction of differentiation for 10 days (n=3), (*p<0.05, **p<0.01) (color online).

peptide (Figure 7(d, e)). These results indicate that the N-cadherin mimetic peptide in the PLG hydrogel promotes chondrogenic differentiation of BMSCs, likely due to the promotion of cell-cell interactions caused by the peptide [38,39]. Furthermore, the results also established the feasibility of using PLG hydrogels grafted with active peptides to regulate cell behavior.

4 Conclusions

In the present study, PLG hydrogels were formed by copper-free click reaction chemistry between PLG-N_3 and PLG-ADIBO under physiological conditions. The gelation time and mechanical properties of the polypeptide hydrogels were adjusted by changing the concentration of the precursor polymer. The PLG hydrogels degraded in the presence of a variety of proteinases. From the cell tests and *in vivo* gelation experiments, it was found that the hydrogels exhibited excellent cytocompatibility *in vitro* and displayed good biocompatibility *in vivo*. Conjugation of RGD to the hydrogels promoted the adhesion and proliferation of BMSCs on the surface of the PLG hydrogels, and also increased the proliferation of BMSCs within the hydrogels in a 3D culture model. In particular, PLG hydrogels modified with both RGD and N-Cad were more conducive to the promotion of chondrogenic differentiation of BMSCs encapsulated within the hydrogels. Therefore, bioactive polypeptide hydrogels represent promising materials for use as scaffolds for cell culture and cartilage tissue engineering.

Acknowledgements This work was supported by the National Natural Science Foundation of China (51973218, 51622307, 21574127, 51520105004) and the Youth Innovation Promotion Association, Chinese Academy of Sciences.

Conflict of interest The authors declare no conflict of interest.

Supporting information The supporting information is available online at http://chem.scichina.com and http://link.springer.com/journal/11426. The supporting materials are published as submitted, without typesetting or editing. The responsibility for scientific accuracy and content remains entirely with the authors.

1 Langer R. *Mol Ther*, 2000, 1: 12–15
2 Lee KY, Mooney DJ. *Chem Rev*, 2001, 101: 1869–1880
3 Moon HJ, Ko DY, Park MH, Joo MK, Jeong B. *Chem Soc Rev*, 2012, 41: 4860
4 Tsou YH, Khoneisser J, Huang PC, Xu X. *Bioactive Mater*, 2016, 1: 39–55
5 Zhong L, Qu Y, Shi K, Chu B, Lei M, Huang K, Gu Y, Qian Z. *Sci China Chem*, 2018, 61: 1553–1567
6 Yu L, Ding J. *Chem Soc Rev*, 2008, 37: 1473
7 Rice JJ, Martino MM, De Laporte L, Tortelli F, Briquez PS, Hubbell JA. *Adv Healthc Mater*, 2013, 2: 57–71
8 Annabi N, Tamayol A, Uquillas JA, Akbari M, Bertassoni LE, Cha C, Camci-Unal G, Dokmeci MR, Peppas NA, Khademhosseini A. *Adv Mater*, 2015, 26: 85–124
9 Xue K, Wang X, Yong PW, Young DJ, Wu YL, Li Z, Loh XJ. *Adv Therap*, 2019, 2: 1800088
10 Lv J, Wu G, Liu Y, Li C, Huang F, Zhang Y, Liu J, An Y, Ma R, Shi L. *Sci China Chem*, 2019, 62: 637–648
11 Deming TJ. *Prog Polym Sci*, 2007, 32: 858–875
12 He C, Zhuang X, Tang Z, Tian H, Chen X. *Adv Healthc Mater*, 2012, 1: 48–78
13 Shirbin SJ, Karimi F, Chan NJA, Heath DE, Qiao GG. *Biomacromolecules*, 2016, 17: 2981–2991
14 Hu C, Liu X, Ran W, Meng J, Zhai Y, Zhang P, Yin Q, Yu H, Zhang Z, Li Y. *Biomaterials*, 2017, 144: 60–72
15 Ren K, He C, Xiao C, Li G, Chen X. *Biomaterials*, 2015, 51: 238–249
16 Ren K, Cui H, Xu Q, He C, Li G, Chen X. *Biomacromolecules*, 2016, 17: 3862–3871
17 Xu Q, He C, Zhang Z, Ren K, Chen X. *ACS Appl Mater Interfaces*, 2016, 8: 30692–30702
18 Zhou X, Li Z. *Adv Healthc Mater*, 2018, 7: 1800020
19 Patel M, Park S, Lee HJ, Jeong B. *Tissue Eng Regen Med*, 2018, 15: 521–530
20 Liu R, Shi Z, Sun J, Li Z. *Sci China Chem*, 2018, 61: 1414–1319
21 Yan S, Zhang X, Zhang K, Di H, Feng L, Li G, Fang J, Cui L, Chen X, Yin J. *J Mater Chem B*, 2016, 4: 947–961
22 Agard NJ, Prescher JA, Bertozzi CR. *J Am Chem Soc*, 2004, 126: 15046–15047
23 Kim E, Koo H. *Chem Sci*, 2019, 10: 7835–7851
24 Madl CM, Katz LM, Heilshorn SC. *Adv Funct Mater*, 2016, 26: 3612–3620
25 Xu J, Filion TM, Prifti F, Song J. *Chem Asian J*, 2011, 6: 2730–2737
26 DeForest CA, Anseth KS. *Annu Rev Chem Biomol Eng*, 2012, 3: 421–444
27 Tibbitt MW, Rodell CB, Burdick JA, Anseth KS. *Proc Natl Acad Sci USA*, 2015, 112: 14444–14451
28 Shi S, Yu SJ, Li G, He CL, Chen XS. *Sci China Technol Sci*, 2020, https://doi.org/10.1007/s11431-019-1466-1
29 Hersel U, Dahmen C, Kessler H. *Biomaterials*, 2003, 24: 4385–4415
30 Leahy DJ, Aukhil I, Erickson HP. *Cell*, 1996, 84: 155–164
31 Yao X, Peng R, Ding J. *Adv Mater*, 2013, 25: 5257–5286
32 DeLise AM, Tuan RS. *J Cell Biochem*, 2002, 87: 342–359
33 Delise AM, Tuan RS. *Dev Dyn*, 2002, 225: 195–204
34 Gumbiner BM. *Nat Rev Mol Cell Biol*, 2005, 6: 622–634
35 Blaschuk OW, Sullivan R, David S, Pouliot Y. *Dev Biol*, 1990, 139: 227–229
36 Williams E, Williams G, Gour BJ, Blaschuk OW, Doherty P. *J Biol Chem*, 2000, 275: 4007–4012
37 Li R, Xu J, Wong DSH, Li J, Zhao P, Bian L. *Biomaterials*, 2017, 145: 33–43
38 Bian L, Guvendiren M, Mauck RL, Burdick JA. *Proc Natl Acad Sci USA*, 2013, 110: 10117–10122
39 Cosgrove BD, Mui KL, Driscoll TP, Caliari SR, Mehta KD, Assoian RK, Burdick JA, Mauck RL. *Nat Mater*, 2016, 15: 1297–1306
40 Kwon MY, Vega SL, Gramlich WM, Kim M, Mauck RL, Burdick JA. *Adv Healthc Mater*, 2018, 7: 1701199
41 Zhao C, Zhuang X, He C, Chen X, Jing X. *Macromol Rapid Commun*, 2008, 29: 1810–1816
42 Cheng Y, He C, Xiao C, Ding J, Zhuang X, Chen X. *Polym Chem*, 2011, 2: 2627
43 Graf N, Bielenberg DR, Kolishetti N, Muus C, Banyard J, Farokhzad OC, Lippard SJ. *ACS Nano*, 2012, 6: 4530–4539
44 Mann T, Leone E. *Biochem J*, 1953, 53: 140–148
45 Chung C, Anderson E, Pera RR, Pruitt BL, Heilshorn SC. *Soft Matter*, 2012, 8: 10141
46 Bian L, Hou C, Tous E, Rai R, Mauck RL, Burdick JA. *Biomaterials*, 2013, 34: 413–421
47 M. Jonker A, A. Bode S, H. Kusters A, van Hest JCM, Löwik DWPM. *Macromol Biosci*, 2015, 15: 1338–1347
48 Even-Ram S, Artym V, Yamada KM. *Cell*, 2006, 126: 645–647
49 Sridhar BV, Brock JL, Silver JS, Leight JL, Randolph MA, Anseth KS. *Adv Healthc Mater*, 2015, 4: 702–713
50 Ren K, He C, Cheng Y, Li G, Chen X. *Polym Chem*, 2014, 5: 5069–5076
51 Park H, Choi B, Hu J, Lee M. *Acta Biomater*, 2013, 9: 4779–4786
52 Qu C, Bao Z, Zhang X, Wang Z, Ren J, Zhou Z, Tian M, Cheng X, Chen X, Feng C. *Int J Biol Macromolecules*, 2019, 125: 78–86
53 Lueckgen A, Garske DS, Ellinghaus A, Mooney DJ, Duda GN, Cipitria A. *Biomaterials*, 2019, 217: 119294
54 Ansari S, Chen C, Xu X, Annabi N, Zadeh HH, Wu BM, Khademhosseini A, Shi S, Moshaverinia A. *Ann Biomed Eng*, 2016, 44: 1908–1920
55 Hong KH, Song SC. *Biomaterials*, 2019, 218: 119338
56 Yang J, Zhang YS, Yue K, Khademhosseini A. *Acta Biomater*, 2017, 57: 1–25